# JAG2 induction in hypoxic tumor cells alters Notch signaling and enhances endothelial cell tube formation

Alexander Pietras[1, 2]*, Kristoffer von Stedingk[1]*, David Lindgren[1], Sven Påhlman[1, 2], and Håkan Axelson[1]

[1]Center for Molecular Pathology and [2]CREATE Health, Department of Laboratory Medicine, Lund University, Skåne University Hospital, Malmö, Sweden

*These authors contributed equally to this work

Correspondence to: Håkan Axelson, Center for Molecular Pathology, Department of Laboratory Medicine, Skåne University Hospital, Entrance 78, SE-205 02 Malmö, Sweden. E-mail: hakan.axelson@med.lu.se; Phone: +46-337621; Fax: +46-40337063

Short title: Hypoxia-induced JAG2 in breast cancer

## Abstract

Several studies have revealed links between hypoxia and activation of Notch in solid tumors. While most reports have focused on icN1 stabilization by direct interaction with HIF proteins, little attention has been given to Notch ligand regulation during hypoxia. Here we show that the Notch ligand *JAG2* is transcriptionally activated by hypoxia in a HIF-1α dependent manner. Hypoxic JAG2 induction resulted in elevated Notch activity in tumor cells, as was measured by increased icN1 levels and induction of the Notch target gene *HEY1*. In primary tumor material, *JAG2* expression correlated with vascular development and angiogenesis gene signatures. In line with this, co-culture experiments of endothelial cells with hypoxic breast cancer cells displayed a reduction in number of capillary-like tubes formed upon *JAG2* siRNA treatment of the breast cancer cells. Together these results suggest that a hypoxic induction of JAG2 in tumor cells mediates a hypoxia-regulated cross-talk between tumor and endothelial cells.

Key words: Notch, Hypoxia, JAG2, Angiogenesis, Breast Cancer

## Introduction

During growth and expansion of solid tumors, the nutrient and oxygen requirements of the expanding tumor generally surpass that being supplied by the supporting vasculature, leading to environmental oxygen shortage (1). This results in a cellular hypoxic response, primarily orchestrated by the hypoxia-inducible factors (HIFs) (2). HIF heterodimers consist of alpha-subunits (HIF-1α and HIF-2α) and the constitutively stable HIF-1β subunit (ARNT). HIF-α and HIF-β subunits heterodimerize within the nucleus where they act as transcription factors, binding to hypoxic response elements (HREs) in HIF target genes such as vascular endothelial growth factor (*VEGF*) (3, 4). Via the induction of *VEGF*, among others, the hypoxic response initiates tumor neo-angiogenesis. This process is a result of endothelial cell proliferation, migration and differentiation along the VEGF gradient produced by the tumor (1). In addition to VEGF regulation of vascular development, branching and expansion of the vasculature are under the control of cell-cell activation of Notch signaling (5). Notch signaling is activated by membrane-bound ligand presentation to a Notch receptor on adjacent cells. Notch ligands include the delta-like and jagged ligands (DLL1, DLL3, DLL4, JAG1 and JAG2, respectively). Interaction of these ligands with one of the Notch receptors (NOTCH1-4) results in γ-secretase-mediated cleavage and release of the intracellular domain of the Notch receptor (icN). icN functions as a nuclear transcription co-factor to activate Notch target genes, such as genes of the Hairy/Enhancer of Split (*HES*) and Hes-related (*HEY*) families of proteins (6), through interaction with the CSL (RBPJ) transcription factor. During vascular development, the Notch ligand DLL4 is of particular importance, since DLL4-mediated

activation of Notch signaling in vasculature results in a process known as lateral inhibition; a process vital for modulating branch formation during angiogenesis (7).

In hypoxic cells cross-talks between HIF and Notch pathways have been reported, primarily resulting in elevated Notch signaling. Several mechanisms have been proposed including direct icN1 stabilization by interaction with HIF proteins (8-18). As of yet, little attention has been given to Notch ligand regulation and the effects this may have on Notch activation under hypoxia. Furthermore, whether hypoxia-induced Notch signaling may influence tumor angiogenesis remains to be investigated. Here we show that hypoxia resulted in elevated expression levels of the Notch ligand *JAG2* via transcriptional activation by HIF-1α. This elevation was responsible for a substantial part of the increased Notch activity observed in hypoxic tumor cells. *JAG2* expression in primary tumor material was correlated with gene signatures of vascular development and angiogenesis. In addition, co-culture of vascular endothelial cells with hypoxic tumor cells revealed that JAG2 expression on tumor cells promoted endothelial cell tube formation. Together these results suggest that a hypoxia regulated cross-talk between tumor and endothelial cells via Notch activation is involved during tumor angiogenesis.

## Materials and Methods

### *Cell Culture*

*Tumor Cells.* MCF7 and T47D cells (ATCC, Manassas, VA) were cultured in RPMI-1640 growth medium, with 10% foetal bovine serum (FBS) and 1% penicillin-streptomycin (PEST). T47D cell medium also contained 1% glucose, 1% sodium

pyruvate, and 5 µl/ml insulin. Under normoxic conditions cells were cultured in a humidified incubator maintained at 37 °C with 5% $CO_2$ and 95% air (approximately 21% $O_2$). Under hypoxic conditions the cells were cultured in a Hypoxystation H35 cell culture incubator, maintained at 37 °C with 1% $O_2$, 5% $CO_2$ and 94% $N_2$.

*Endothelial Cells.* MS1 murine endothelial cells were cultured at the same normoxic conditions as described above in EBM-2 medium (Lonza, Basel, Switzerland) supplemented with EGM-2 MV SingleQuots (Lonza; (hydrocortisone, hEGF, FBS, VEGF, hFGFB, R3-IGF-1, ascorbic acid and gentamicin/amphotericin-B). The cell culture plates were coated with 1% gelatin.

***siRNA Transfections for QPCR and Protein Analysis***

Cells were seeded out into 6 well plates (2 wells per si-treatment) at a density of 120 000 cells per well. The cells were left to attach overnight. The cell medium (as described above) was removed and replaced with 2 ml Optimem (Invitrogen, Paisley, UK) without any added FBS or antibiotics. Lipofectamin 2000 (Invitrogen) was used as the transfection agent. Pre-designed Silencer Select siRNAs (Ambion, Austin, TX), were used to silence desired genes. Tranfections were carried out with a Lipofectamin 2000 concentration of 1.5 µl/ml, and siRNA concentrations ranging from 2.5 nM to 10 nM. Cells were tranfected under normoxic conditions (described above) for 6 hour. The transfection medium was then replaced with respective cell mediums (described above) containing 10% FBS and no antibiotics. Cells were maintained in normoxic culture overnight. Cells were then moved to respective oxygen conditions (21% or 1% $O_2$) and cultured for 24 hours before harvesting.

***siRNA Transfections for co-culture experiments***

Cells were seeded out into as above at a density of 200 000 cells per well. Cells were left to attach overnight. The transfection procedure was carried out as above. Following the 6 hour transfection, the transfection medium was replaced with respective cell mediums (described above), and the cells were moved to respective oxygen conditions (21% or 1% $O_2$). The cells were cultured over-night before seeding in the co-culture experiments.

***Chromatin Immunoprecipitation (ChIP)***

T47D cells were cultured under hypoxia for 24 hours. Cells were then harvested and immunoprecipitation was performed using the Diagenode Transcription Factor ChIP Kit according to protocol. In brief, the cells were fixed and collected using the scraping method. This was followed by cell lysis in 1x proteosome inhibitor containing lysis buffer. Chromatin shearing was then performed using a Diagenode Bioruptor sonicator set on high for 7.5 cycles of 30 seconds at 4 °C. Immunoprecipitation was performed using either anti-human IgG antibody (rabbit polyclonal, Abcam, Cambridge, UK) or anti-human HIF-1α antibody (rabbit polyclonal – ChIP grade, Abcam). Precipitated protein-DNA complexes were then de-cross-linked by overnight incubation at 65 °C in a thermoshaker. DNA was purified using phenol extraction and used for quantitative real-time PCR using primers specific for a potential HIF binding sites within the *JAG2* promoter (Supplementary Data Table 1B). Primers targeting the known HRE within the *VEGF* promoter were used as the positive control, and primers targeting a region upstream of the *JAG2* promoter were used as a negative control (Supplementary Data

Table 1B). Relative precipitated DNA values were calculated using the Delta-Delta-CT method.

***Quantitative real-time PCR***

Cells were lysed and homogenized using the QIAshredder kit (Qiagen, Sollentuna, Sweden), then loaded onto RNeasy spin columns (Qiagen) for total RNA extraction according to the manufacturer's recommendation. After DNAse treatment and extensive washing using Microcon spin columns, cDNA was synthesized using random primers and Multiscribe Reverse Transcriptase enzyme (Applied Biosystems, Foster City, CA). Generated cDNA was used as template with SYBR Green PCR Master Mix (Applied Biosystems) and expression levels were quantified using the comparative Ct method. Expression levels were normalized using the expression of three housekeeping genes (*UBC*, *YWHAZ* and *SDHA*) (19). Primer sequences are listed in Supplementary Data Table 1A.

***Western blot***

For protein extraction, cells were pelleted by centrifugation, then lysed in 10 mM Tris-HCL (pH 7.2), 160 mM NaCl, 1% Triton X-100, 1% sodium deoxycholate, 0.1% SDS, 1 mM EGTA, 1 mM EDTA (RIPA) supplemented with Complete Protease Inhibitor cocktail (Roche Molecular Biochemicals, Bromma, Sweden). The method of Bradford was used to determine protein concentrations. SDS-PAGE separation of proteins in MOPS buffer (Invitrogen) and subsequent blotting onto PVDF membranes (Millipore, Billerica, MA) was done using the NuPAGE gels and system (Invitrogen) according to

the manufacturer's instructions. Membrane blocking and antibody dilutions were made in 5% milk diluted in 0.010 M phosphate buffer (pH 7.4), 2.7 mM KCl, 0.140 M NaCl, 0.05% Tween®20 (PBS-Tween). The following antibodies and antisera were used: Actin (MP Biomedicals; diluted 1:2000), Intracellular Notch-1 (Cell Signaling, Beverly, MA; diluted 1:500), JAG2 (Abcam; diluted 1:400), sheep anti-mouse and anti-rabbit secondary antibodies (GE Healthcare, Uppsala, Sweden; diluted 1:5000).

***Immunohistochemistry and immunofluorescence***

For immunohistochemistry, human ductal carcinoma in situ (DCIS) specimens were routinely embedded in paraffin upon fixation. The Envision system and DAKO Techmate 500 were used for detection of protein after incubation of sections with the following primary antibodies: HIF-1α (Upstate; diluted 1:100), JAG2 (Abcam; diluted 1:250)

For immunofluorescence, cells were grown on cover slips and then fixed in 4% paraformaldehyde. After blocking in 5% normal goat serum and 0.3% Triton X-100 in PBS for 30 minutes, cover slips were incubated for 1 h with JAG2 antisera (Abcam; diluted 1:400) diluted in PBS, then washed and further incubated for 1 h with secondary antibody conjugated to Alexa fluor 488 (Molecular Probes). Cover slips were mounted in PVA-DABCO.

***Endothelial cell tube formation***

Ten thousand MS1 (transformed mouse pancreatic islet endothelial) cells (20) (a kind gift from Dr. Kristian Pietras, Karolinska Institutet, Stockholm, Sweden) were mixed with

$10^4$ T47D breast cancer cells (treated as indicated), then seeded in 96 well plates on top of a layer of growth factor-reduced Matrigel (BD) in EBM-2 medium (Lonza) supplemented with EGM-2 MV SingleQuots (Lonza; (hydrocortisone, hEGF, FBS, VEGF, hFGFB, R3-IGF-1, ascorbic acid and gentamicin/amphotericin-B). Matrigel was thawed slowly at 4 °C over night, then allowed to polymerize at 37 °C for 30 minutes before seeding. Tube formation and length was measured using three photographs from each group taken at 8 h post-seeding. For number of tubes formed, each connected tube in each photograph was counted and average values within groups were compared. For measurements of tube length, images were first processed using the ImageJ software and the Tubeness plugin (21) to visualize tubes. Each tube was then identified and total tube length quantified using the Fiji software (http://pacific.mpi-cbg.de/wiki/index.php/Main_Page) and the Simple neurite tracer plugin (http://homepages.inf.ed.ac.uk/s9808248/imagej/tracer/). In both cases, values were normalized to the average value in cells cultured with untransfected T47D cells and statistical significance calculated using a one-way ANOVA followed by Tukey HSD test comparing the control transfected group with JAG2 siRNA groups. For conditioned media experiments, siRNA treated T47D cells were cultured in EBM2 medium over night under hypoxia, after which MS1 cells were seeded as above with conditioned media replacing the T47D cells.

***Nuclear extracts***

Nuclei were extracted after harvesting cells in 40 mM Tris-Cl pH 7.5, 1 mM EDTA, 150 mM NaCl (TEN), then washed in PBS and 25 mM Tris pH 7.5, 50 mM KCl, 2 mM

$MgCl_2$, 1 mM EDTA, 5 mM Dithiotreitol (DTT) (Buffer A). Pellets were resuspended in 25 mM Tris pH 7.5, 0.42 M NaCl, 1.5 mM $MgCl_2$, 0.5 mM EDTA, 1 mM Dithiotreitol (DTT), 25 % Sucrose (Buffer NE) and nuclei extracted for 30'. After centrifugation to remove cellular debris, supernatants were used as the nuclear fraction.

***Gene expression analysis***

JAG2 expression data from Chi et al. (22) were analyzed using Oncomine (23). For the JAG2 correlation analyses in primary tumor material two gene expression data sets, the first comprising 200 breast tumors (24) and a second comprising 59 clear cell renal carcinoma samples (25) were downloaded from the NCBI GEO website [http://www.ncbi.nlm.nih.gov/geo/] (accession numbers GSE11121 and GSE14994, respectively). Raw CEL-files were RMA normalized in R [http://www.r-project.org] using the Affy package. For both of these data sets, the Pearson correlation was calculated between JAG2 expression and all other reporters present on the array. Genes were then ranked according to their respective JAG2 correlations and GSEA (26) was applied on these ranked lists using the c2.v2.5 curated gene sets collection as supplied by the Molecular Signatures Database [MSigDB, broad.mit.edu/gsea/msigdb]. Gene Ontology analyses were performed on the 100 reporters showing highest correlation to JAG2 using the Functional Annotation Tool in DAVID (27, 28) and on the complete ranked JAG2 correlation lists using the c5.v2.5 GO gene sets collection in GSEA.

JAG2 expression in hypoxic MCF7 cells treated with siRNA targeting HIF1A and/or HIF2A was obtained from the previously published dataset by Elvidge et al. (29). This dataset was downloaded from the NCBI GEO website with accession number GSE3188.

## Results

### Notch signaling is enhanced by hypoxia

MCF7 and T47D breast cancer cell lines were cultured at 21% or 1% oxygen (normoxia and hypoxia respectively) for 24 h. In both cell lines, exposure to hypoxia resulted in increased nuclear icN1 protein levels as indicated by western blot analysis using an antibody specific for the activated intracellular domain of the Notch1 receptor (Fig. 1A). In conjunction with the increased icN1 levels, expression of the known Notch target gene *HEY1* (30) was also substantially elevated, as revealed by quantitative real-time PCR (QPCR) (Fig. 1B). These results are in agreement with the notion that hypoxia enhances Notch signaling.

### *JAG2* is transcriptionally activated under hypoxia

In order to determine potential factors responsible for the increased Notch activation observed under hypoxia, the expression of all Notch receptors and ligands in breast cancer cells were examined using QPCR both at normoxia and hypoxia (Fig. 1C-D). With regards to the Notch receptors, *NOTCH1, NOTCH2* and *NOTCH4* did not appear to be transcriptionally regulated by hypoxia, but *NOTCH3* displayed increased transcript levels (Fig. 1C). It has previously been shown that NOTCH3 can be involved in regulating the activity of icN1 and downstream NOTCH targets (31, 32), and can therefore not be excluded from having an influence on icN1 elevation in hypoxia nor effects on overall NOTCH signaling.

The increase in cleaved icN1 levels could also potentially be attributed to changes in Notch ligand expression. Expression analyses revealed that although all Notch ligands, with the exception of *DLL3*, which fell below detection limits, appeared up-regulated under hypoxia, only *JAG2* levels were significantly increased (Fig. 1D). Notably, the detection level of the Notch ligand *JAG2* was a minimum of five PCR cycles lower than that of all other ligands, suggesting highest expression levels of *JAG2* amongst the Notch ligands.

**JAG2 is induced by hypoxia in vivo and in vitro in different tissues/cells**

To confirm that the increase in *JAG2* observed at the transcriptional level corresponded to an increase at the protein level, JAG2 protein expression was examined by immunofluorescence in T47D cells cultured at normoxia or hypoxia. The hypoxic T47D cells displayed an evident induction of JAG2 protein when compared to those grown at normoxia (Fig. 2A). The detected JAG2 protein appeared to be primarily localized to the cellular membrane (Fig. 2A, inset), as was expected for a functional Notch ligand. In addition, immunohistochemistry was performed on sections of breast ductal carcinoma *in situ* (DCIS) specimens, which in the *comedo* form are characterized by necrotic cores with surrounding hypoxic cells (33). JAG2 protein expression was elevated in the hypoxic regions of the tumor surrounding the necrotic cores (Fig. 2B), which was confirmed by detection of HIF-1α protein in the same peri-necrotic regions.

In order to determine if the hypoxic induction of *JAG2* was specific to breast cancer or if it could be detected in other cellular systems, expression data from hypoxia-treated cells

were examined using the online database Oncomine (23). Here it was found that for both mammary epithelial and renal proximal tubule epithelial cells (22), exposure to hypoxia resulted in increased levels of *JAG2* (Fig. 2C). Furthermore, microarray data from macrophage and Burkitt's lymphoma cells as well as QPCR data on neuroblastoma cells cultured at normoxia and hypoxia demonstrated a consistent upregulation of *JAG2* mRNA levels under hypoxic conditions (Fig. 2D).

Moreover, we analysed a dataset from a microarray performed on 200 breast cancers (24) as well as a dataset consisting of 59 renal cell carcinomas (RCC) (25). For each dataset, all genes present on the arrays were ranked according to their correlation to *JAG2* expression. Gene set enrichment analysis (GSEA) was then applied on the resulting *JAG2* correlation ranked gene lists. Consistent in both the breast cancer and RCC arrays, the ranked lists displayed significant enrichment of hypoxia up-regulated gene signatures (Fig. 2E, Supplementary Table 2) (FDR q-value=0.009, NES: 1.99; breast cancer and FDR q-value<0.000, NES: 2.32; RCC). Together these data show that hypoxia consistently results in increased *JAG2* mRNA and protein levels in a variety of cell types, both *in vivo* and *in vitro*, and that *JAG2* expression in both breast cancer and RCC correlated with transcriptional responses observed under hypoxia, suggesting that *JAG2* induction is a general phenomenon in hypoxic cells.

### *JAG2* up-regulation by hypoxia is HIF dependent

To determine if the hypoxic induction of *JAG2* was HIF dependent, T47D cells were cultured under hypoxia and treated with siRNAs targeting either *HIF1A* or *HIF2A* (Fig.

3A-B). *JAG2* levels were then monitored using QPCR showing that knockdown of *HIF1A*, but not *HIF2A*, diminished *JAG2* expression under hypoxia to levels near that detected at normoxia (Fig. 3C). In addition, a publicly available microarray dataset on MCF7 cells treated with siRNAs targeting *HIF1A* and/or *HIF2A* under hypoxia (29) also displayed a marked reduction in *JAG2* levels upon *HIF1A* but not *HIF2A* silencing (Fig. 3D). To further confirm HIF-1α involvement in *JAG2* induction, chromatin immunoprecipitation experiments were performed on T47D cells cultured under hypoxia for 24 h. As a positive control, HIF-1α pull-down on a previously defined *VEGF*-HRE (34) displayed a 5-fold enrichment compared to the background IgG pull-down (Fig. 3E), and as a negative control, a region upstream of the *JAG2* promoter displayed no apparent enrichment (Fig. 3E). After screening a variety of potential HREs located within the promoter region of *JAG2*, HIF-1α pull-down yielded a 12-fold enrichment over the negative control IgG. HIF-1α was found to bind strongest within a sequence ranging from 1229 to 1328 base-pairs downstream of the starting ATG of the *JAG2* promoter, with a potential HRE at the +1294 position (Fig. 3F). This identified a potential HIF-1α responsive HRE within the *JAG2* gene, as well as identified *JAG2* as a direct HIF target gene.

**JAG2 contributes to the enhanced Notch activity observed under hypoxia**

Taking into consideration the elevated Notch signaling observed during hypoxia, the role of JAG2 in hypoxic Notch activation was investigated. T47D cells treated with siRNA targeting *JAG2* were cultured in normoxia or hypoxia. The *JAG2* knockdown was confirmed at both mRNA and protein levels under hypoxia (Fig. 4A-B). To examine the

effects of diminished JAG2 levels on Notch signaling, icN1 protein levels were again examined by western blot. The knockdown of *JAG2* resulted in a substantial decrease in nuclear icN1 protein levels present under hypoxia (Fig. 4C). In addition, the Notch target gene *HEY1* also displayed marked reduction in its hypoxic up-regulation upon *JAG2* depletion (Fig. 4D). Considering the reduction in both cleaved NOTCH1 levels and hypoxic *HEY1* induction, JAG2 elevation strongly contributed to the increase in Notch activity observed under hypoxia.

### *JAG2* expression signature in primary tumor material significantly correlates with angiogenic processes

To further investigate which functional processes are associated with *JAG2* expression in primary cancer materials, a gene ontology (GO) analysis was performed on the 100 array reporters showing highest correlation to *JAG2* expression. Interestingly, in both breast cancer and RCC arrays, several angiogenic ontology terms were significantly enriched among the *JAG2* correlated genes (Table 1A-B), including processes such as blood vessel morphogenesis, blood vessel development, vascular development, and angiogenesis. GO analysis was also performed on the full *JAG2* correlation ranked lists using GSEA, again displaying enrichments for vascular development (Fig. 5A-B, Supplementary Table 2) and angiogenesis (Fig. 5A-B, Supplementary Table 2) in both datasets (FDR q-value=0.009, NES: 1.97; breast cancer vascular development; FDR q-value=0.023, NES: 1.86; breast cancer angiogenesis; FDR q-value=0.04, NES: 1.79; RCC vascular development; FDR q-value=0.05, NES: 1.75; RCC angiogenesis).

**Hypoxic JAG2 expression in epithelial tumor cells contributes to endothelial cell tube formation**

Since Notch signaling has a pivotal role in endothelial cell angiogenesis and recent work has displayed interactions between tumor epithelial cells and their surrounding vascular endothelial cells (35), we next investigated whether epithelial JAG2 upregulation under hypoxia might have a direct role in regulating tumor angiogenesis. To investigate this, an *in vitro* co-culture system was employed. T47D cells treated with control or *JAG2* siRNA were cultured under hypoxia for 18 h prior to being seeded onto Matrigel in combination with the murine-derived endothelial cells MS1 (20). The tube formation capacity of the endothelial cells was then examined (Fig. 6A). Interestingly, depletion of *JAG2* from the epithelial T47D cell population resulted in a significant reduction in MS1 cell tube formation measured as number of tubes formed as well as total tube length (Fig. 6B-C). This reduction appeared cell-cell contact dependent, as MS1 cells grown with conditioned medium from siRNA treated hypoxic T47D cells displayed no significant change in tube formation between groups (Fig. 6D).

## Discussion

It has been previously reported that Notch signaling is elevated during hypoxia (8, 10, 11, 14, 18). Here we show that a substantial part of this elevation can be attributed to increased expression of the Notch ligand JAG2. The hypoxic induction of *JAG2* was HIF dependent, and we show HIF binding to a potential HRE downstream of the *JAG2* start codon. In human tumors, JAG2 protein levels were elevated in hypoxic regions of the

tumor, and GSEA analysis revealed that *JAG2* expression is correlated with hypoxic gene signatures in primary breast cancer and RCC material.

Until now, reports on Notch activity in hypoxia have largely focused on intracellular interactions between icN and HIFs, resulting in enhanced transcription of Notch downstream targets (8, 10). Even though our results showed that JAG2 was responsible for a large fraction of the Notch activity under hypoxia, silencing of *JAG2* did not result in complete inhibition of the hypoxic potentiation of Notch signaling. In light of the previous reports, the remaining elevation in Notch activity could be due to direct HIF-icN1 interactions or elevation of other Notch receptors (36).

The development of a hypoxic environment inevitably results in initiation of angiogenesis and recruitment of new blood vessels. It has been shown that hypoxic cells secrete VEGF among other growth factors, creating a VEGF gradient between the hypoxic source and the surrounding vasculature (1). The vasculature is then activated by the secreted factors and extends in the direction of the VEGF gradient (37). The mechanism behind the extension/formation of the new vasculature has been a recent subject of intense interest and has led to development of VEGF inhibitors for anti-angiogenic tumor therapies. Recent studies have also unveiled the pivotal importance of Notch signaling in the process of angiogenesis, with specific focus on two Notch ligands *DLL4* and *JAG1* (5, 38-42). It is suggested that branching of new vasculature is a result of modulation of Notch signaling within the endothelial cells. Activation of endothelial cells via secreted VEGF stimulation results in up-regulation of *DLL4*, which in turn activates

Notch in adjacent cells in a ligand dependant manner (7). The VEGF stimulated DLL4-high endothelial cell, termed the "tip-cell", direct the branching along the VEGF gradient. Meanwhile, the adjacent Notch-activated cells, termed the "stalk-cells", become less responsive to VEGF via down-regulation of VEGF-receptors, and instead take on the proliferative role driving new vascular formation (7). In addition, stalk-cells also up-regulate the Notch ligand JAG1 that, in contrast to the Notch activating role of DLL4, results in inhibition of Notch-activation back on the tip-cell (42). In total, this results in a mechanism in which tip-cells with low Notch-activity drive the branching of new vasculature, whereas stalk-cells with high Notch-activity drive the lengthening of the vessels. This mechanism is supported by multiple studies in which inhibition of Notch signaling during vascular development results in a hyper-branching phenotype (38-41, 43).

Considering the known involvement on Notch in the process of angiogenesis, we speculated that hypoxic induction of *JAG2* and its influence on Notch signaling could represent a novel mechanism for tumor induced vasculogenesis. Upon conducting a GO analysis on primary breast and RCC tumors, highly significant correlations between *JAG2* expression and genes involved in angiogenic processes were detected. This was further confirmed by performing a GSEA on complete *JAG2* correlated-ranked lists, again displaying significant enrichment for vascular development and angiogenesis gene signatures. In addition, co-culture experiments using hypoxic breast cancer epithelial cells and murine endothelial cells displayed significantly reduced endothelial tube formation as was measured by both number of branches and length of tubes.

Interestingly, it has previously been shown in head and neck squamous cell carcinoma that growth factor-induced JAG1 expression on tumor cells resulted in increased tumor vascularisation (35). It was hypothesized that this increase in angiogenic processes was a result of an increase in endothelial Notch-activity due to JAG1 stimulation. However, in light of recent work displaying an inhibitory role of JAG1 on Notch-activity in endothelial cells (42), it seems probable that the increased vascular branching could be attributed to Notch-inhibition as apposed to activation. In line with this model, our co-culture experiments also suggest vascular branching due to alterations to endothelial Notch activation via JAG2 stimulation, which according to what is known today, is likely to be a Notch-inhibiting effect. Our findings bring to light the possibility of local tumor cell-endothelial cell activating cues functioning in a juxtacrine manner that would contribute to tumor endothelial cell angiogenesis in addition to the paracrine stimulation via VEGF.

**Conflicts of interest**

The authors declare no conflicts of interest.

**Acknowledgments**

We thank Elise Nilsson and Siv Beckman for skillful technical assistance and Dr. Kristian Pietras, Karolinska Institutet, Stockholm, Sweden, for providing the MS1 cells.

**Financial disclosure**

This work was supported by the Swedish Cancer Society, the Children Cancer Foundation of Sweden, the Swedish Research Council, the Swedish Foundation for Strategic Research supported Strategic Center for Translational Cancer Research, CREATE Health, the Strategic Cancer Research Program, BioCARE, Ollie and Elof Ericsson's, Crafoord's, Gunnar Nilsson's foundations, and the research funds of Malmö University Hospital. The funders had no role in study design, data collection and analysis, decision to publish, or preparation of the manuscript.

## References

1. Carmeliet P, Jain RK. Angiogenesis in cancer and other diseases. Nature 2000; 407: 249-57.
2. Semenza GL. Targeting HIF-1 for cancer therapy. Nat Rev Cancer 2003; 3: 721-32.
3. Harris AL. Hypoxia--a key regulatory factor in tumour growth. Nat Rev Cancer 2002; 2: 38-47.
4. Holmquist-Mengelbier L, Fredlund E, Löfstedt T, et al. Recruitment of HIF-1alpha and HIF-2alpha to common target genes is differentially regulated in neuroblastoma: HIF-2alpha promotes an aggressive phenotype. Cancer Cell 2006; 10: 413-23.
5. Thurston G, Noguera-Troise I, Yancopoulos GD. The Delta paradox: DLL4 blockade leads to more tumour vessels but less tumour growth. Nat Rev Cancer 2007; 7: 327-31.
6. Artavanis-Tsakonas S, Rand MD, Lake RJ. Notch signaling: cell fate control and signal integration in development. Science 1999; 284: 770-6.
7. Phng LK, Gerhardt H. Angiogenesis: a team effort coordinated by notch. Dev Cell 2009; 16: 196-208.
8. Gustafsson MV, Zheng X, Pereira T, et al. Hypoxia requires notch signaling to maintain the undifferentiated cell state. Dev Cell 2005; 9: 617-28.
9. Zheng X, Linke S, Dias JM, et al. Interaction with factor inhibiting HIF-1 defines an additional mode of cross-coupling between the Notch and hypoxia signaling pathways. Proc Natl Acad Sci U S A 2008; 105: 3368-73.
10. Sahlgren C, Gustafsson MV, Jin S, Poellinger L, Lendahl U. Notch signaling mediates hypoxia-induced tumor cell migration and invasion. Proc Natl Acad Sci U S A 2008; 105: 6392-7.
11. Jögi A, Ora I, Nilsson H, et al. Hypoxia alters gene expression in human neuroblastoma cells toward an immature and neural crest-like phenotype. Proc Natl Acad Sci U S A 2002; 99: 7021-6.

12. Pietras A, Hansford LM, Johnsson AS, et al. HIF-2alpha maintains an undifferentiated state in neural crest-like human neuroblastoma tumor-initiating cells. Proc Natl Acad Sci U S A 2009; 106: 16805-10.
13. Pistollato F, Rampazzo E, Persano L, et al. Interaction of HIF1alpha and Notch Signaling Regulates Medulloblastoma Precursor Proliferation and Fate. Stem Cells 2010.
14. Bar EE, Lin A, Mahairaki V, Matsui W, Eberhart CG. Hypoxia increases the expression of stem-cell markers and promotes clonogenicity in glioblastoma neurospheres. Am J Pathol 2010; 177: 1491-502.
15. Eliasz S, Liang S, Chen Y, et al. Notch-1 stimulates survival of lung adenocarcinoma cells during hypoxia by activating the IGF-1R pathway. Oncogene 2010; 29: 2488-98.
16. Yustein JT, Liu YC, Gao P, et al. Induction of ectopic Myc target gene JAG2 augments hypoxic growth and tumorigenesis in a human B-cell model. Proc Natl Acad Sci U S A 2010; 107: 3534-9.
17. Main H, Lee KL, Yang H, et al. Interactions between Notch- and hypoxia-induced transcriptomes in embryonic stem cells. Exp Cell Res 2010; 316: 1610-24.
18. Chen J, Imanaka N, Griffin JD. Hypoxia potentiates Notch signaling in breast cancer leading to decreased E-cadherin expression and increased cell migration and invasion. Br J Cancer 2010; 102: 351-60.
19. Vandesompele J, De Preter K, Pattyn F, et al. Accurate normalization of real-time quantitative RT-PCR data by geometric averaging of multiple internal control genes. Genome Biol 2002; 3: RESEARCH0034.
20. Arbiser JL, Moses MA, Fernandez CA, et al. Oncogenic H-ras stimulates tumor angiogenesis by two distinct pathways. Proc Natl Acad Sci U S A 1997; 94: 861-6.
21. Sato Y, Nakajima S, Shiraga N, et al. Three-dimensional multi-scale line filter for segmentation and visualization of curvilinear structures in medical images. Med Image Anal 1998; 2: 143-68.
22. Chi JT, Wang Z, Nuyten DS, et al. Gene expression programs in response to hypoxia: cell type specificity and prognostic significance in human cancers. PLoS Med 2006; 3: e47.
23. Rhodes DR, Yu J, Shanker K, et al. ONCOMINE: a cancer microarray database and integrated data-mining platform. Neoplasia 2004; 6: 1-6.
24. Schmidt M, Bohm D, von Torne C, et al. The humoral immune system has a key prognostic impact in node-negative breast cancer. Cancer Res 2008; 68: 5405-13.
25. Beroukhim R, Brunet JP, Di Napoli A, et al. Patterns of gene expression and copy-number alterations in von-hippel lindau disease-associated and sporadic clear cell carcinoma of the kidney. Cancer Res 2009; 69: 4674-81.
26. Subramanian A, Tamayo P, Mootha VK, et al. Gene set enrichment analysis: a knowledge-based approach for interpreting genome-wide expression profiles. Proc Natl Acad Sci U S A 2005; 102: 15545-50.
27. Huang da W, Sherman BT, Lempicki RA. Systematic and integrative analysis of large gene lists using DAVID bioinformatics resources. Nat Protoc 2009; 4: 44-57.
28. Dennis G, Jr., Sherman BT, Hosack DA, et al. DAVID: Database for Annotation, Visualization, and Integrated Discovery. Genome Biol 2003; 4: P3.
29. Elvidge GP, Glenny L, Appelhoff RJ, Ratcliffe PJ, Ragoussis J, Gleadle JM. Concordant regulation of gene expression by hypoxia and 2-oxoglutarate-dependent

dioxygenase inhibition: the role of HIF-1alpha, HIF-2alpha, and other pathways. J Biol Chem 2006; 281: 15215-26.
30. Maier MM, Gessler M. Comparative analysis of the human and mouse Hey1 promoter: Hey genes are new Notch target genes. Biochem Biophys Res Commun 2000; 275: 652-60.
31. Beatus P, Lundkvist J, Oberg C, Lendahl U. The notch 3 intracellular domain represses notch 1-mediated activation through Hairy/Enhancer of split (HES) promoters. Development 1999; 126: 3925-35.
32. Ohashi S, Natsuizaka M, Yashiro-Ohtani Y, et al. NOTCH1 and NOTCH3 coordinate esophageal squamous differentiation through a CSL-dependent transcriptional network. Gastroenterology; 139: 2113-23.
33. Helczynska K, Kronblad A, Jogi A, et al. Hypoxia promotes a dedifferentiated phenotype in ductal breast carcinoma in situ. Cancer Res 2003; 63: 1441-4.
34. Lofstedt T, Jogi A, Sigvardsson M, et al. Induction of ID2 expression by hypoxia-inducible factor-1: a role in dedifferentiation of hypoxic neuroblastoma cells. J Biol Chem 2004; 279: 39223-31.
35. Zeng Q, Li S, Chepeha DB, et al. Crosstalk between tumor and endothelial cells promotes tumor angiogenesis by MAPK activation of Notch signaling. Cancer Cell 2005; 8: 13-23.
36. Sansone P, Storci G, Giovannini C, et al. p66Shc/Notch-3 interplay controls self-renewal and hypoxia survival in human stem/progenitor cells of the mammary gland expanded in vitro as mammospheres. Stem Cells 2007; 25: 807-15.
37. Gerhardt H. VEGF and endothelial guidance in angiogenic sprouting. Organogenesis 2008; 4: 241-6.
38. Hellstrom M, Phng LK, Hofmann JJ, et al. Dll4 signalling through Notch1 regulates formation of tip cells during angiogenesis. Nature 2007; 445: 776-80.
39. Ridgway J, Zhang G, Wu Y, et al. Inhibition of Dll4 signalling inhibits tumour growth by deregulating angiogenesis. Nature 2006; 444: 1083-7.
40. Noguera-Troise I, Daly C, Papadopoulos NJ, et al. Blockade of Dll4 inhibits tumour growth by promoting non-productive angiogenesis. Nature 2006; 444: 1032-7.
41. Siekmann AF, Lawson ND. Notch signalling limits angiogenic cell behaviour in developing zebrafish arteries. Nature 2007; 445: 781-4.
42. Benedito R, Roca C, Sorensen I, et al. The notch ligands Dll4 and Jagged1 have opposing effects on angiogenesis. Cell 2009; 137: 1124-35.
43. Haller BK, Brave A, Wallgard E, et al. Therapeutic efficacy of a DNA vaccine targeting the endothelial tip cell antigen delta-like ligand 4 in mammary carcinoma. Oncogene 2010; 29: 4276-86.
44. Bostrom P, Magnusson B, Svensson PA, et al. Hypoxia converts human macrophages into triglyceride-loaded foam cells. Arterioscler Thromb Vasc Biol 2006; 26: 1871-6.
45. Kim JW, Tchernyshyov I, Semenza GL, Dang CV. HIF-1-mediated expression of pyruvate dehydrogenase kinase: a metabolic switch required for cellular adaptation to hypoxia. Cell Metab 2006; 3: 177-85.

**Figure Legends**

*Figure 1:* Notch signaling is elevated in hypoxia. MCF7 and T47D breast cancer cells were cultured in normoxia (21% oxygen) and hypoxia (1% oxygen). A. Western blot analysis of activated *NOTCH1* (icN1) on nuclear extracts. B. QPCR analysis of mRNA expression levels of *HEY1*. Expression levels are displayed as relative expression levels to those observed in normoxia. Data represent 1 of at least 3 independent experiments run in triplicate. Error bars represent SD. C. Relative mRNA levels of the Notch receptors (*NOTCH1-4*). D. Relative mRNA levels of the Notch ligands (*DLL1, DLL4, JAG1, JAG2*). *DLL3* transcript levels are not displayed due to Ct levels being below the detection cut-off of 35. Average normoxic Ct values obtained from QPCR analysis are displayed. Error bars represent SD. Data represent mean values from 3 independent experiments run in triplicate. * indicates $p<0.05$, ** indicates $p<0.01$, in a two-tailed unpaired Student's t-test.

*Figure 2:* JAG2 protein and mRNA levels are elevated by hypoxia in vivo and in vitro in different tissues/cells. A. Immunofluorescence staining of JAG2 protein in T47D cells cultured at normoxia or hypoxia. Inset shows immunohistochemical staining of JAG2 in hypoxic T47D cells. B. Immunohistochemical analysis of a breast ductal carcinoma *in* situ. Antibodies recognizing HIF-1α (left) and JAG2 (right) were used. * indicates areas magnified in insets. C. *JAG2* mRNA expression from public microarray datasets obtained from Oncomine. Expression analysis was performed on mammary epithelial cells (left) and renal proximal tubule epithelial cells (right) that had been cultured at normoxia, hypoxia or anoxia. D. *JAG2* mRNA expression from public microarray datasets on

cultured human macrophages (44) and P493-6 Burkitt's lymphoma cells (45) and QPCR data on cultured human neuroblastoma SK-N-BE(2)C cells at normoxia and hypoxia as indicated. Error bars represent SD. E. Gene set enrichment analyses (GSEAs) of hypoxia-up-regulated gene set performed on *JAG2* correlated ranked gene lists produced from microarray analyses of 200 breast tumors (left) (FDR q-value=0.009, NES: 1.99) or 59 RCCs (right) (FDR q-value<0.000, NES: 2.32).

*Figure 3:* Hypoxic *JAG2* induction is HIF dependent. T47D cells were cultured at 21% or 1% oxygen and were treated with control siRNA or siRNA targeting *HIF1A* or *HIF2A* (A,B,C). mRNA levels were then examined using QPCR and presented as relative expression compared to normoxic levels. A. Relative mRNA levels of *HIF1A*. Data represent mean values from 3 independent experiments run in triplicate. Error bars represent SD. B. Relative mRNA levels of *HIF2A*. Data represent mean values from 3 independent experiments run in triplicate. Error bars represent SD. C. Relative mRNA levels of *JAG2*. Data represent mean values from 3 independent experiments run in triplicate. Error bars represent SD. * indicates $p<0.05$ in a two-tailed unpaired Student's t-test. D. *JAG2* levels in hypoxic MCF7 cells treated with siRNA targeting *HIF1A* and/or *HIF2A* as indicated, from data published in (29). Error bars represent SD. E. Chromatin immunoprecipitation of potential HRE located down-stream of the *JAG2* starting ATG performed on T47D cells cultured under hypoxia for 24 h. Pull-downs were performed using anti-human IgG (negative control) and anti-human HIF-1α. *VEGF*-promoter was used as a positive control and a non-enriched region in the *JAG2* promoter as a negative control for the HIF-1α pull-down. Graph displays fold enrichment of precipitated DNA

relative to background IgG-pulled DNA. Data represent mean values from 2 independent experiments run in triplicate. Error bars represent SD of the fold enrichment. F. A schematic representation of the potential HRE within *JAG2*. The sequence of the potential HIF-binding site is displayed and is present at the +1294 position.

Figure 4: JAG2 modulates Notch signaling under hypoxia. T47D cells were cultured at 21% or 1% oxygen and were treated with control siRNA or siRNA targeting *JAG2*. A. Relative mRNA levels of *JAG2* were examined using QPCR and presented as relative expression compared to normoxic levels. Data represent mean values from 3 independent experiments run in triplicate. Error bars represent SD. B. Western blot analysis of JAG2 in control and *JAG2* siRNA treated hypoxic T47D cells. C. Western blot analysis of icN1 on nuclear extracts from untreated, control and *JAG2* siRNA treated hypoxic T47D cells. D. QPCR derived relative mRNA levels of *HEY1*, displayed as relative quantities compared to control treated normoxic T47D cells. Data represent mean values from 3 independent experiments run in triplicate. Error bars represent SD. * indicates $p<0.05$, in a two-tailed unpaired Student's t-test.

*Figure 5: JAG2* correlated gene expression displays enrichment for angiogenic processes. A. GSEAs performed on a *JAG2* correlated ranked gene list produced from a microarray examining gene expression in 200 breast cancers. Significant enrichments were observed for both vascular development (left) (FDR q-value=0.009, NES: 1.97) and angiogenesis (right) (FDR q-value=0.023, NES: 1.86) gene signatures. B. GSEAs performed on a *JAG2* correlated ranked gene list produced from a microarray examining gene expression

in 70 renal cell carcinomas. Enrichments were observed for both vascular development (left) (FDR q-value=0.04, NES: 1.79) and angiogenesis (right) (FDR q-value=0.05, NES: 1.75) gene signatures.

*Figure 6:* Tumor cell JAG2 expression influences endothelial cell tube formation. T47D cells were pre-cultured under hypoxia and treated with control siRNA or siRNA targeting *JAG2*. Hypoxia treated T47D cells were then co-cultured with MS1 endothelial cells. A. One representative light-microscopy image of co-culture tube formation under different T47D siRNA treatments. B. Number of tubes formed in each co-culture, expressed as relative number compared to non-siRNA treated co-cultures. Error bars represent SD of the mean values from 3 independent experiments. C. Length of tubes formed in each co-culture, expressed as relative number compared to non-siRNA treated co-cultures. Error bars represent SD of the mean values from 3 independent experiments. D. Number of tubes formed in each MS1 culture with media conditioned by hypoxic T47D cells over night as indicated. Error bars represent SD of the mean values form 3 independent experiments. * indicates $p<0.05$, in a one-way ANOVA ($p=0.007$) followed by a Tukey HSD test.

Figure 1

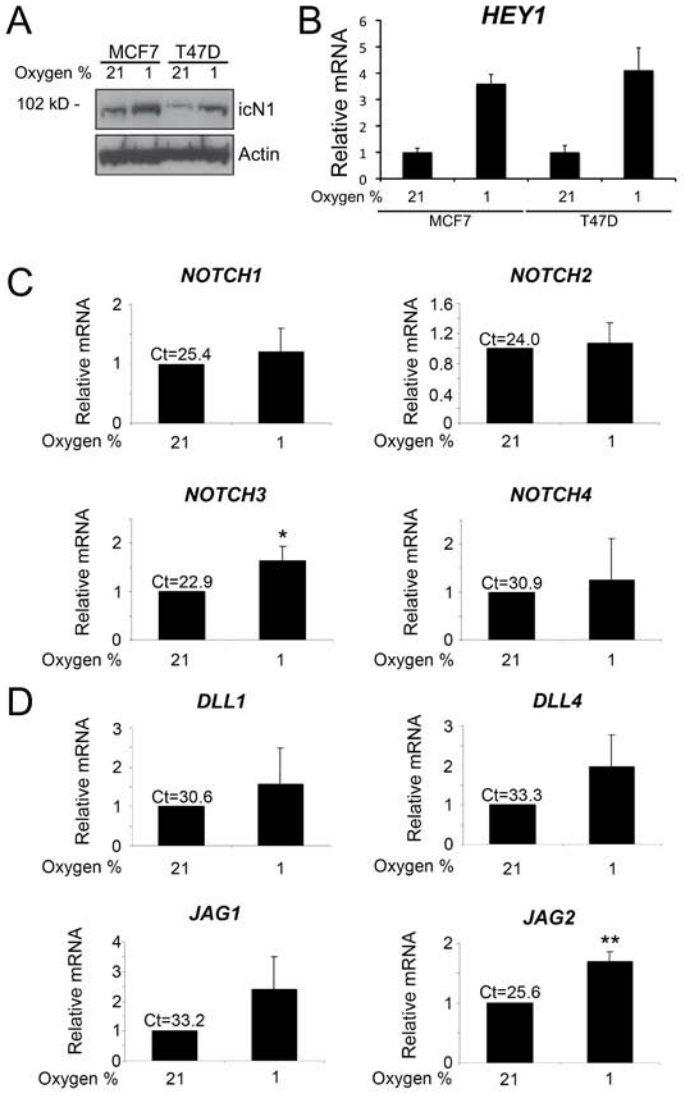
A
MCF7
T47D
Oxygen %
21
1
21
1
102 kD -
icN1
Actin
B
HEY1
Relative mRNA
Oxygen %
21
1
21
1
MCF7
T47D
C
NOTCH1
Ct=25.4
NOTCH2
Ct=24.0
NOTCH3
Ct=22.9
*
NOTCH4
Ct=30.9
D
DLL1
Ct=30.6
DLL4
Ct=33.3
JAG1
Ct=33.2
JAG2
Ct=25.6
**

Figure 2

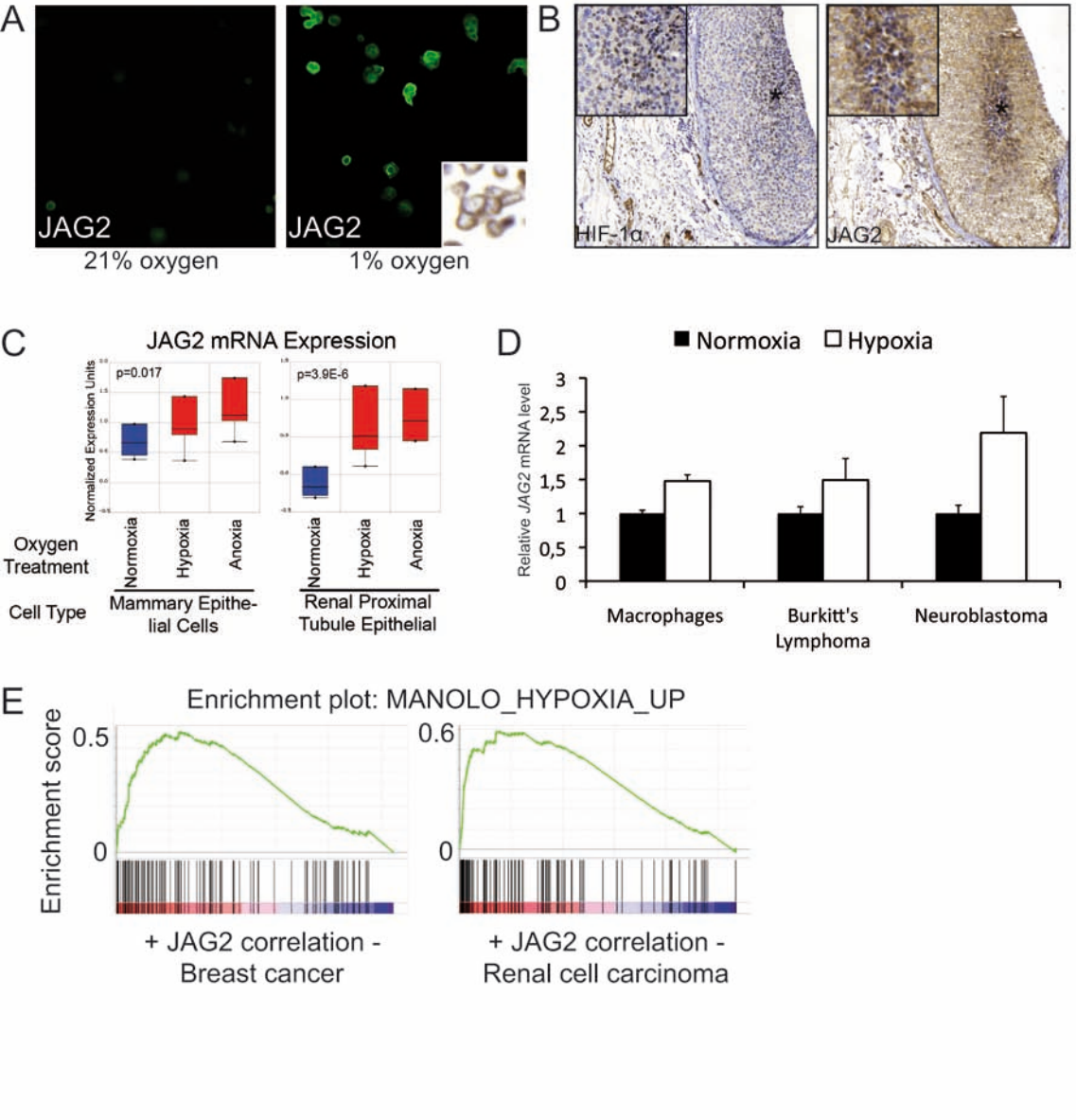
A
JAG2
21% oxygen
JAG2
1% oxygen
B
HIF-1α
JAG2
C
JAG2 mRNA Expression
Normalized Expression Units
p=0.017
p=3.9E-6
Normoxia
Hypoxia
Anoxia
Oxygen Treatment
Cell Type
Mammary Epithelial Cells
Renal Proximal Tubule Epithelial
D
Normoxia
Hypoxia
Relative JAG2 mRNA level
3
2,5
2
1,5
1
0,5
0
Macrophages
Burkitt's Lymphoma
Neuroblastoma
E
Enrichment plot: MANOLO_HYPOXIA_UP
Enrichment score
0.5
0
0.6
0
+ JAG2 correlation - Breast cancer
+ JAG2 correlation - Renal cell carcinoma

Figure 3

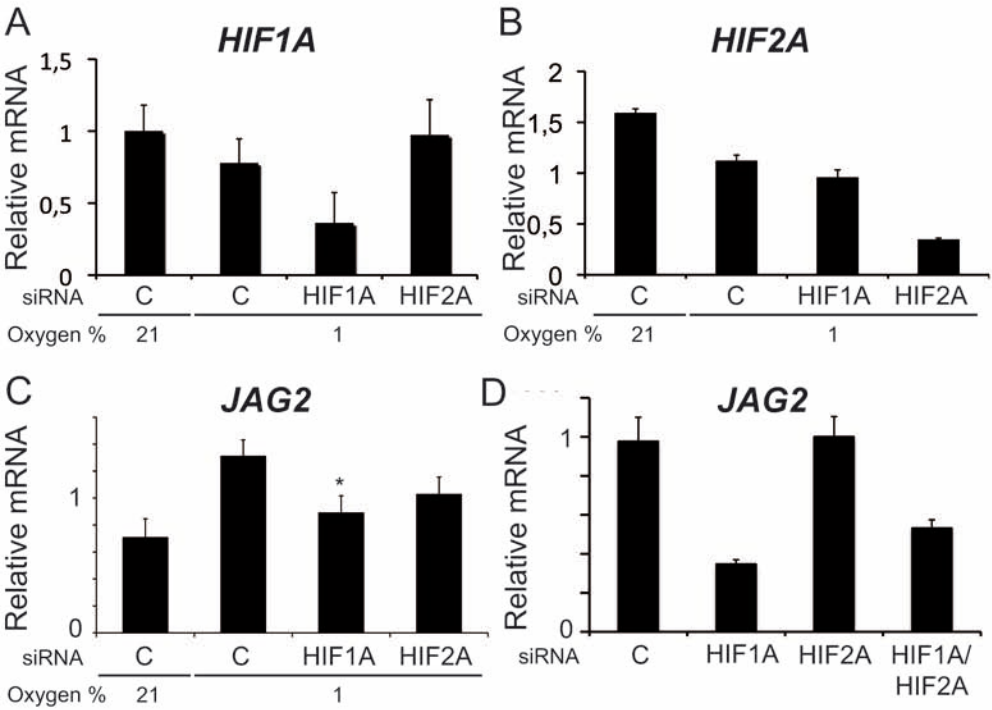
A
HIF1A
Relative mRNA
1,5
1
0,5
0
siRNA
C
C
HIF1A
HIF2A
Oxygen %
21
1
B
HIF2A
Relative mRNA
2
1,5
1
0,5
0
siRNA
C
C
HIF1A
HIF2A
Oxygen %
21
1
C
JAG2
Relative mRNA
1
0
*
siRNA
C
C
HIF1A
HIF2A
Oxygen %
21
1
D
JAG2
Relative mRNA
1
0
siRNA
C
HIF1A
HIF2A
HIF1A/
HIF2A

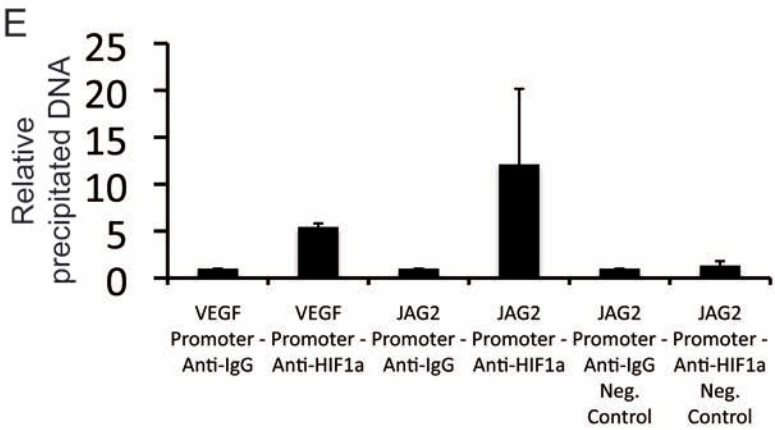
E
Relative precipitated DNA
25
20
15
10
5
0
VEGF Promoter - Anti-IgG
VEGF Promoter - Anti-HIF1a
JAG2 Promoter - Anti-IgG
JAG2 Promoter - Anti-HIF1a
JAG2 Promoter - Anti-IgG Neg. Control
JAG2 Promoter - Anti-HIF1a Neg. Control


F
JAG2 --
ATG
JAG2-HRE
GGCGTG +1294

Figure 4

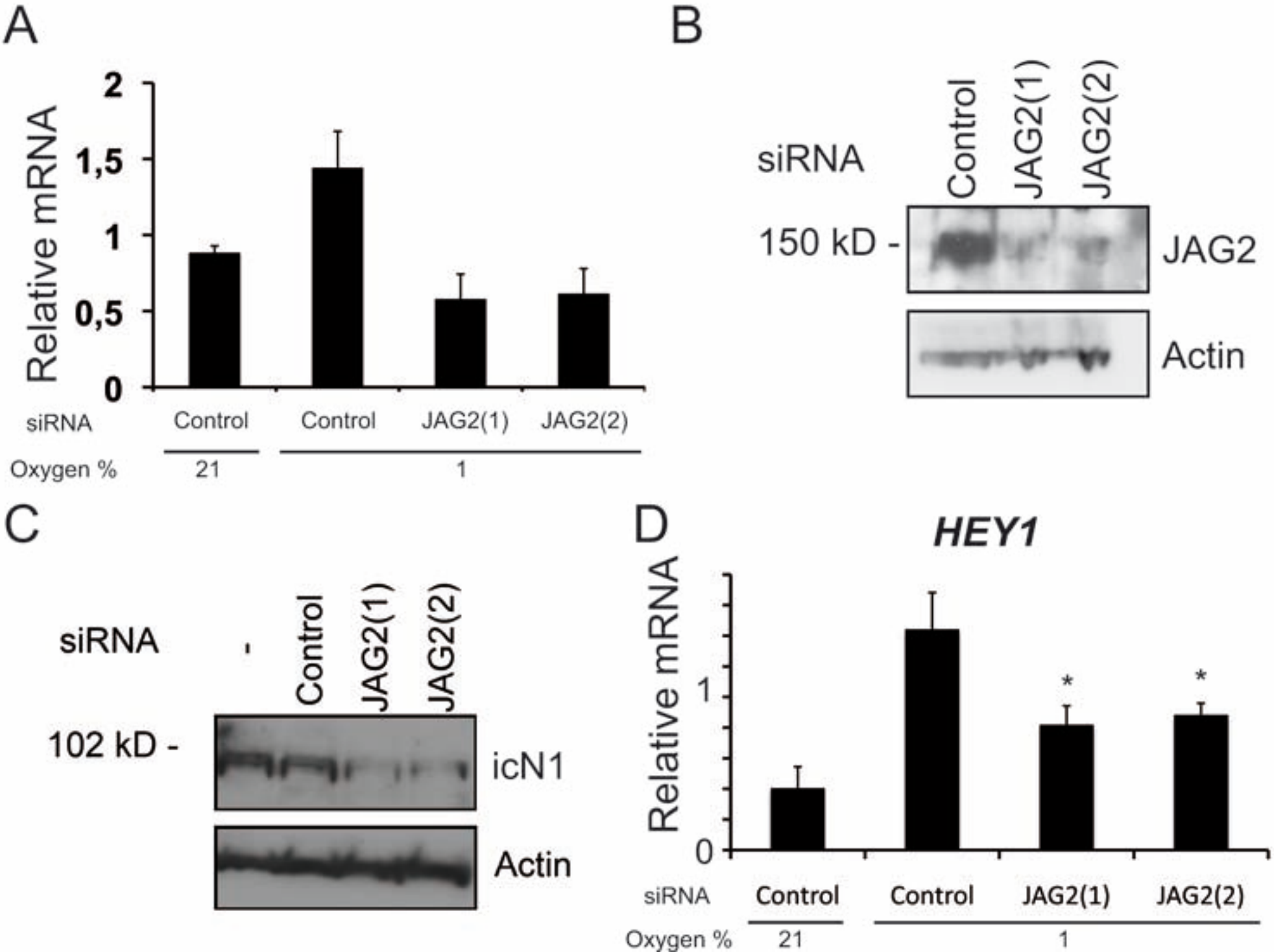
A
Relative mRNA
2
1,5
1
0,5
0
siRNA
Control
Control
JAG2(1)
JAG2(2)
Oxygen %
21
1
B
siRNA
Control
JAG2(1)
JAG2(2)
150 kD -
JAG2
Actin
C
siRNA
-
Control
JAG2(1)
JAG2(2)
102 kD -
icN1
Actin
D
HEY1
Relative mRNA
1
0
*
*
siRNA
Control
Control
JAG2(1)
JAG2(2)
Oxygen %
21
1

Figure 5

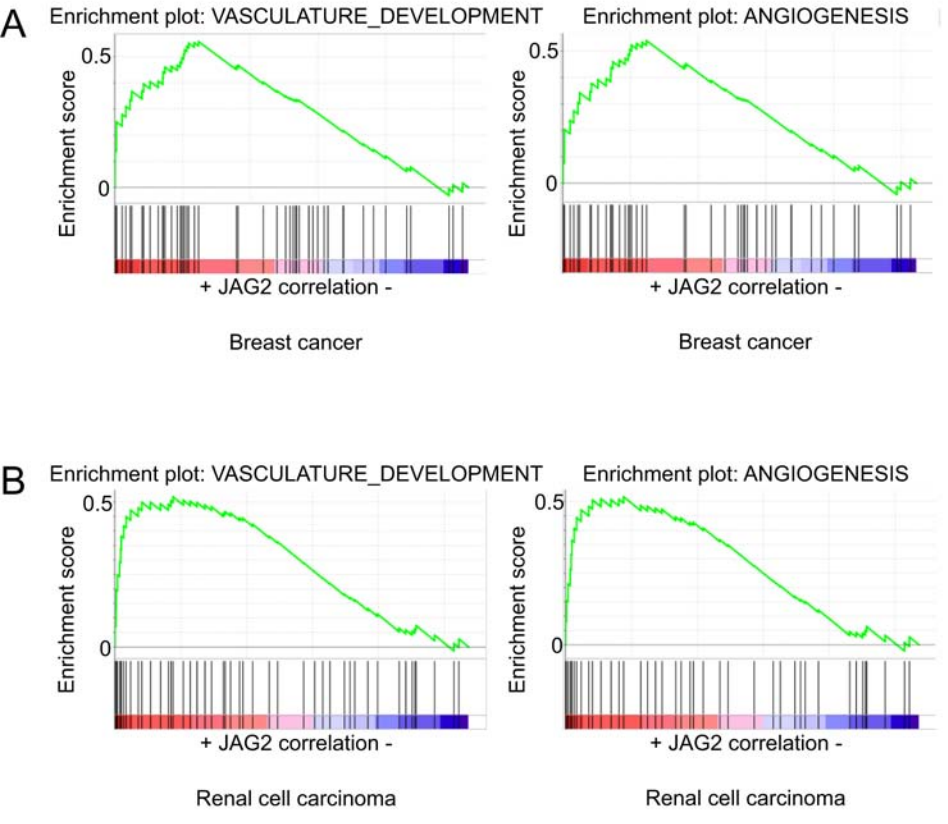
A
Enrichment plot: VASCULATURE_DEVELOPMENT
Enrichment score
0.5
0
+ JAG2 correlation -
Breast cancer
Enrichment plot: ANGIOGENESIS
Enrichment score
0.5
0
+ JAG2 correlation -
Breast cancer
B
Enrichment plot: VASCULATURE_DEVELOPMENT
Enrichment score
0.5
0
+ JAG2 correlation -
Renal cell carcinoma
Enrichment plot: ANGIOGENESIS
Enrichment score
0.5
0
+ JAG2 correlation -
Renal cell carcinoma

Figure 6

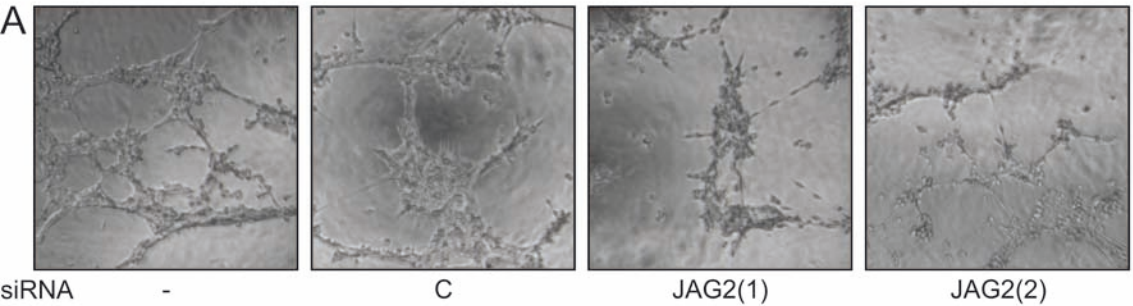
A
siRNA
-
C
JAG2(1)
JAG2(2)

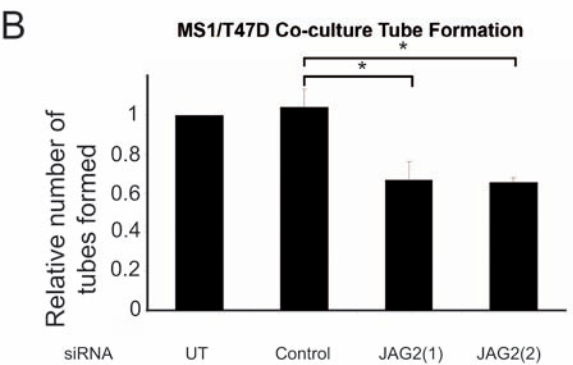
B
MS1/T47D Co-culture Tube Formation
Relative number of tubes formed
0
0.2
0.4
0.6
0.8
1
*
*
siRNA
UT
Control
JAG2(1)
JAG2(2)

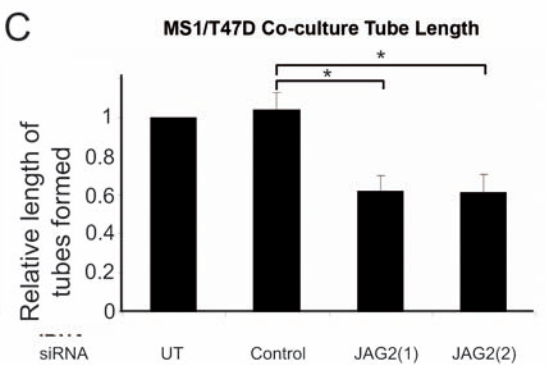
C
MS1/T47D Co-culture Tube Length
Relative length of tubes formed
0
0.2
0.4
0.6
0.8
1
*
*
siRNA
UT
Control
JAG2(1)
JAG2(2)

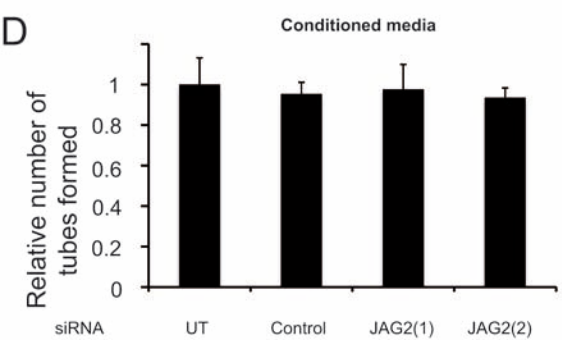
D
Conditioned media
Relative number of tubes formed
0
0.2
0.4
0.6
0.8
1
siRNA
UT
Control
JAG2(1)
JAG2(2)

*Table 1*. JAG2 expression significantly correlates with angiogenic processes. A. Gene ontology analysis performed on the top 100 JAG2 correlated gene list produced from a microarray examining gene expression in 200 breast cancers B. Gene ontology analysis performed on the top 100 JAG2 correlated gene list produced from a microarray examining gene expression in 59 renal cell carcinomas.

A

| Enrichment Score:4.85 | | |
|---|---|---|
| **Correlated Processes** | **P value** | **Benjamini (Corrected P value)** |
| **Blood Vessel Morphogenesis** | 6.0E-8 | **3.1E-4** |
| **Blood Vessel Development** | 1.7E-7 | **4.6E-4** |
| **Vascular Development** | 2.0E-7 | **3.5E-4** |
| **Angiogenesis** | 2.7E-7 | **3.5E-4** |
| **Anatomical Structure Development** | 1.2E-6 | **1.3E-3** |
| **Anatomical Structure Formation** | 1.5E-6 | **1.3E-3** |
| **Anatomical Structure Morphogenesis** | 2.1E-6 | **1.6E-3** |
| **Organ Development** | 2.9E-6 | **1.9E-3** |
| **Developmental Process** | 4.0E-6 | **2.3E-3** |
| **Organ Morphogenesis** | 1.7E-5 | **9.1E-3** |
| **Multicellular Organismal Development** | 6.4E-5 | **2.6E-2** |
| **System Development** | 7.7E-5 | **2.8E-2** |
| **Multicellular Organismal Process** | 1.3E-3 | 2.2E-1 |
| **Biological Regulation** | 4.3E-3 | 4.7E-1 |
| **Regulation of Biological Process** | 6.7E-3 | 6.0E-1 |
| **Regulation of Cellular Process** | 2.9E-2 | 9.5E-1 |

B

| Enrichment Score:6.12 | | |
|---|---|---|
| **Correlated Processes** | **P value** | **Benjamini (Corrected P value)** |
| **Blood Vessel Development** | 1.1E-14 | **5.8E-11** |
| **Vascular Development** | 1.4E-14 | **3.6E-11** |
| **Blood Vessel Morphogenesis** | 1.5E-12 | **2.7E-9** |

| | | |
|---|---|---|
| **Angiogenesis** | 4.0E-9 | **5.3E-6** |
| **Organ Morphogenesis** | 5.5E-9 | **5.8E-6** |
| **Anatomical Structure Development** | 6.2E-9 | **5.4E-6** |
| **Organ Development** | 6.4E-9 | **4.8E-6** |
| **Anatomical Structure Formation** | 2.9E-8 | **1.9E-5** |
| **Anatomical Structure Morphogenesis** | 2.9E-8 | **1.7E-5** |
| **Multicellular Organismal Development** | 4.1E-8 | **2.2E-5** |
| **System Development** | 3.3E-7 | **1.4E-4** |
| **Developmental Process** | 7.6E-7 | **3.1E-4** |
| **Multicellular Organismal Process** | 1.4E-6 | **5.3E-4** |
| **Angiogenesis** | 2.5E-5 | **4.5E-3** |